Delft University of Technology

Joint Use of Drone-Mounted Base Stations and Cell Outage Compensation in Emergency Scenarios

Pijnappel, T. R.; Van Den Berg, J. L.; Borst, S. C.; Litjens, R.

Important note
To cite this publication, please use the final published version (if applicable).
Please check the document version above.

Joint Use of Drone-Mounted Base Stations and Cell Outage Compensation in Emergency Scenarios

T.R. Pijnappel[*], J.L. van den Berg[†], S.C. Borst[*], R. Litjens[§‡]

[*]Eindhoven University of Technology, Eindhoven, The Netherlands
[†]University of Twente, Enschede, The Netherlands
[§]TNO, The Hague, The Netherlands
[‡]Delft University of Technology, Delft, The Netherlands

Abstract—Under normal circumstances wireless cellular networks provide adequate coverage and capacity. However in case of site failures, due to for example an earthquake or flooding, it is important to quickly resolve the resulting coverage and/or capacity problem. To achieve this goal, we investigate the joint use of dynamically deployed drone-mounted base stations (DBSs) and a cell outage compensation (COC) mechanism. With COC the surrounding, still operational, cells adjust their configuration to mitigate the performance degradation. We demonstrate that these two approaches can work well together and complement each other in the sense that while COC on its own is usually unable to restore the performance to its original level, it can help to significantly reduce the number of DBSs required to achieve this. In particular, in urban scenarios we observe a reduction in the number of DBSs to be deployed by up to 40%.

Index Terms—5G, drone base station positioning, cell outage compensation, data-driven algorithms, emergency scenarios

I. INTRODUCTION

Wireless cellular networks play an essential role in today's digital society. They are carefully planned to provide adequate coverage and sufficient capacity to support a wide range of applications. However, in emergency scenarios like earthquakes or floodings, part of the network may become inoperative and consequently unable to provide satisfactory service. In such scenarios it is of critical importance that these issues are resolved quickly and efficiently. For this purpose, network operators can use a feature known as *cell outage compensation (COC)* which is capable of automatically adjusting a variety of control parameters in the cells surrounding a site failure, including the reference signal power or antenna tilt [1]. Alternatively, operators can consider the temporary deployment of *drone-mounted base stations (DBSs),* which function as regular base stations, but can dynamically adjust their positions to provide service in areas where it is needed most [2].

The use of COC algorithms has been studied in several papers of which we present a selection here. These COC mechanisms often adjust *(i)* the antenna tilts [1], [3]–[6] and/or *(ii)* power-related settings, e.g. the reference signal transmit power or the target uplink received power level) [1], [3], [5]–[9]. A range of algorithmic approaches is used to adjust such configuration parameters, e.g. Q-learning [6], particle swarm

optimization [8], fuzzy logic [5], threshold-based approaches [1], [3] and several other approaches [4], [7], [9].

The effective use of DBSs crucially depends on their positioning. Suitably positioned DBSs can significantly improve network performance, by providing additional coverage and/or capacity. However, ill-positioned DBSs potentially even degrade network performance as they cause additional interference. Several papers consider the DBS positioning problem, e.g. [10], [11] propose a Q-learning solution, [12], [13] uses particle swarm optimization, while yet other approaches are proposed by [14]–[18], all aiming to find the optimal positions of the DBSs for fixed user constellations. The work in [19] and [20] propose DBS positioning algorithms that account for dynamically changing user populations.

While the listed papers all consider either the positioning of the DBSs or the use of COC mechanisms, to the best of our knowledge this is the first paper exploring the potential gains from the *joint* use of these approaches in case of site failures. In particular, distinguishing between urban and rural scenarios, we conduct an extensive simulation study to investigate to what extent the network performance in terms of the call success rate (CSR) can be restored after one or more site failures and how this depends on the parameter settings of the interacting control algorithms. It is shown that with proper parameter settings COC and dynamic DBS positioning work well together and complement each other. Specifically, while COC on its own is mostly unable to restore the CSR to its original level, it can help to reduce the number of DBSs required to achieve this by up to 40% in urban scenarios.

The remainder of this paper is organized as follows. Section II introduces the main modeling assumptions. In Section III we describe the considered scenarios and performance metric. Section IV outlines the DBS positioning algorithm as well as the COC algorithm. In Section V we provide an overview of the results, followed by conclusions in Section VI.

II. MODELING ASSUMPTIONS

In order to evaluate the performance jointly achieved by the proposed DBS positioning and COC algorithms, we conduct extensive simulation experiments. An overview of the key underlying modeling assumptions regarding network and antenna aspects, propagation characteristics, data traffic characteristics

and resource management are given in the respective subsections below.

A. Network and antenna aspects

We assume a hexagonal network layout of twelve three-sectorized sites comprising $12 \times 3 = 36$ cells. We make a distinction between capacity-limited and coverage-limited scenarios, which we characterize by the assumption of an urban and a rural environment with inter-site distances (ISDs) of 500 m and 3500 m, respectively. We use a wraparound feature to mimic an infinite-size network and avoid boundary effects. Each (regular) cell is served by a directional antenna located at a height of 25 m and 35 m for the urban and rural deployments, respectively [21, Table 7.4.1-1]. For the antenna gains we use the model proposed in [22], which is characterized by the horizontal and vertical half-power beam widths HPBW$_{h,v}$ (in degrees), the maximum gain G_r (in dBi), the front back ratio FBR (in dB) and the side lobe level SLL (in dB). Given these, we can express the total antenna gain as $G(\varphi, \theta) = G_h(\varphi) + G_v(\theta)$ where

$$G_h(\varphi) = -\min \left\{ 12 \left(\frac{\varphi}{\text{HPBW}_h} \right)^2, \text{FBR}_h \right\} + G_r, \quad (1)$$

$$G_v(\theta) = \max \left\{ -12 \left(\frac{\theta - \theta_{\text{etilt}}}{\text{HPBW}_v} \right)^2, \text{SLL}_v \right\}, \quad (2)$$

where φ denotes the horizontal angle relative to the azimuth direction, θ denotes the negative elevation angle relative to the horizontal plane and θ_{etilt} denotes the electrical downtilt, set to $7°$ and $4°$ for urban and rural environments, respectively. Each cell is assigned a $B = 5$ MHz carrier in the 3.5 GHz band with a fraction $\kappa = 0.25$ of the carrier resources used for control signaling and a transmit power of $P_r^{\max} = 20$ W.

We consider a deployment of a given number of DBSs, which are assumed to be wirelessly backhauled on a distinct carrier frequency. For the antenna gain of the DBSs we assume that DBSs are equipped with an antenna consisting of a single antenna element. We then use a rotated version of the model provided in [21, Table 7.3-1], adapting the vertical component to ensure a circular footprint. As a result we model the antenna gain using the following formula

$$G(\varphi) = -\min \left\{ 12 \left(\frac{\varphi}{\text{HPBW}_d} \right)^2, A_{\max} \right\} + G_d, \quad (3)$$

with $A_{\max} = 30$ dB the maximum attenuation and G_d the maximum gain (both in dB). We assume the DBSs are assigned the same frequency carrier as the regular cells, but with a transmit power of $P_d^{\max} = 0.5$ W. See Table I for all applied antenna parameters, based on [23].

B. Propagation characteristics

For the link between regular cells and UEs we use the path loss models provided in [21, Tables 7.4.1 and 7.4.2]. We determine the path loss as the weighted average of the path loss for a line-of-sight (LoS) and a non-line-of-sight (NLoS)

link, with weights given by the probability of having a LoS or NLoS link.

In view of the higher altitude and different orientation of the DBSs, we use a different path loss model for links between DBSs and UEs, characterised by three statistical parameters to reflect different kinds of scattering environments [24]:

α: the ratio of built-up land area to the total land area;
β: the number of buildings per square kilometer;
γ: a scale parameter of a Rayleigh distribution describing the buildings' heights.

Using these parameters we can determine two other environment parameters ξ and ψ as detailed in [25]. We can then formulate the path loss between the DBS and a UE as the free-space path loss plus an excessive path loss component η_{LoS} or η_{NLoS} (depending on the type of link), given by [25]:

$$L_d = 20 \log_{10} \left(\frac{4\pi df}{c} \right) + p_{\text{LoS}} \eta_{\text{LoS}} + (1 - p_{\text{LoS}}) \eta_{\text{NLoS}}, \quad (4)$$

where c denotes the speed of light, f the carrier frequency and d the 3D-distance between the DBS and the UE, and

$$p_{\text{LoS}} = 1 - p_{\text{NLoS}} = \frac{1}{1 + \xi \exp\left(-\psi[\arctan(h/r) - \xi]\right)}, \quad (5)$$

with h and r the height difference and the horizontal distance between the UE and the DBS, respectively.

Besides the path loss, the propagation loss of a signal is also affected by shadow fading. To incorporate this, we determine spatially and site-to-site correlated shadow fading maps for each of the sites according to the model provided in [26]. For this model we need to specify three parameters: the site-to-site correlation $\omega = 0.5$, the decorrelation distance $d_{\text{decorr}} = 45$ and 80 m, and the standard deviation of the shadow fading $\sigma_{\text{sh}} = 5$ and 6 dB for urban and rural environments, respectively.

Lastly, we impose a minimum coupling loss of 70 and 80 dB for the urban and rural environment, respectively [27]. See Table I for the other applied propagation parameters, based on [21] and [28].

C. Traffic characteristics

We assume that call initiations by UEs occur according to a spatially uniform Poisson process with rate λ, set to 1.3 and 0.018 calls/s/km^2 for the urban and rural environment, respectively. We further assume the emergence of a traffic hotspot caused by a network disruption event. This hotspot area is assumed to be a circle with radius of 100 m, where the arrival rate of new calls is ρ times higher than elsewhere. The value of ρ and the location of the traffic hotspot will be varied in the different simulation scenarios.

All active UEs are assumed to be static and have a height of 1.5 m. The calls are assumed to have an exponentially distributed duration with a mean of $\tau = 120$ seconds. We further assume that all calls require a minimum bit rate of $R = 0.4$ Mb/s for their entire duration.

D. Resource management aspects

Upon call generation, we determine the Reference Signal Received Power (RSRP) to all cells and verify whether the associated UE has coverage or not, i.e. whether any of the RSRPs exceeds the coverage threshold of -120 dBm. When the UE has coverage, it is assigned to the covering cell with the highest value of RSRP+CIO, with CIO the configured cell individual offset, i.e. a cell selection bias. The assigned cell's admission control mechanism then estimates the fraction of downlink resources this new call requires in support of its minimum required bit rate R. The required fraction of the serving cell's resources is estimated by $R/((1-\kappa)B\log_2(1+\text{SINR}))$, where SINR denotes the estimated Signal-to-Interference-plus-Noise Ratio of the new UE. We assume a thermal noise of -106.94 dBm and a receiver noise figure of 8 dB. The admission control mechanism admits the new call when sufficient resources can be made available without violating the minimum bit rate requirement of on-going calls.

In line with the aim to optimize the call success rate (defined in detail below), we assume a scheduling mechanism that allocates a cell's available resources in a proportional fair way subject to the minimum bit rate requirements. In the unfortunate case where it is not possible to provide all served UEs with their required minimum bit rate (which may be caused by DBS movements), as many UEs as possible receive their required amount of resources. Any remaining resources are then given to the unsatisfied UE that requires the least amount of resources.

The dynamic adjustments of the DBSs positions lead to changes in the experienced path losses and antenna gains. As a consequence, the total amount of resources required in a cell may exceed the available capacity, in which case at least one UE no longer receives its minimum required bit rate. Another consequence is that the RSRP values change as well, which can lead to handover requests when the RSRP + CIO of a candidate target cell exceeds the RSRP+CIO of the currently serving cell by at least 3 dB (hysteresis value) for at least 200 ms (time to trigger). When such a handover request is submitted to the target cell, the admission control treats this request in the same way as it treats a new UE. Whenever a handover request is denied, it is repeated after 50 ms provided that the conditions triggering the handover are still satisfied. In an extreme case, the RSRP changes may cause a loss of coverage and, consequently, a dropped call.

## III. SCENARIOS AND PERFORMANCE METRIC

We consider a wide range of scenarios, determined by the type of environment (dense urban or rural, denoted by DU and RU, respectively), the number of failing sites N_{failing}, the location of the hotspot (defined by the angular orientation ϕ_{hotspot} w.r.t. the horizontal axis and the distance d_{hotspot} w.r.t. the red-marked reference site in Figure 1a) and the previously introduced relative hotspot traffic intensity ρ. To enable easy references we denote a given scenario by $\{\text{DU}, \text{RU}\}$-N_{failing}-ϕ_{hotspot}-d_{hotspot}-ρ. For example, the DU-1-60-150-4 scenario assumes a dense urban environment with a single failing site,

Table I: Antenna and propagation parameters.

Parameter	Urban	Rural	Unit
G_r	15.4	15.4	dBi
HPBW_h	72	72	°
HPBW_v	5.6	5.6	°
FBR_h	24	24	dB
SLL_v	-11	-11	dB
G_d	8	8	dBi
HPBW_d	65	65	°
α	0.5	0.05	
β	300	300	buildings/km^2
γ	20	4	
η_{LoS}	1.7	0.1	dB
η_{NLoS}	24	22	dB

a traffic hotspot located at 150 m from the failing site along the line that makes a $60°$ angle with the horizontal axis, with a relative traffic intensity of $\rho = 4$.

We adopt the call success rate (CSR) as our key performance metric, which incorporates both coverage and capacity. A call is deemed successful if the associated UE has coverage, the call is admitted to the system, is not dropped and receives its minimally required bit rate throughout its entire duration. It is important to specify the geographical area over which the CSR is evaluated. In case of one or more site failures, the cells surrounding the failing sites take over part of the traffic that would normally be served by these failing sites. We therefore evaluate the CSR for the area comprised by the cells of the failing sites and the cells adjacent to them, including any coverage gaps in this area, depicted by the blue and green shaded cells in Figures 1a-1b, respectively.
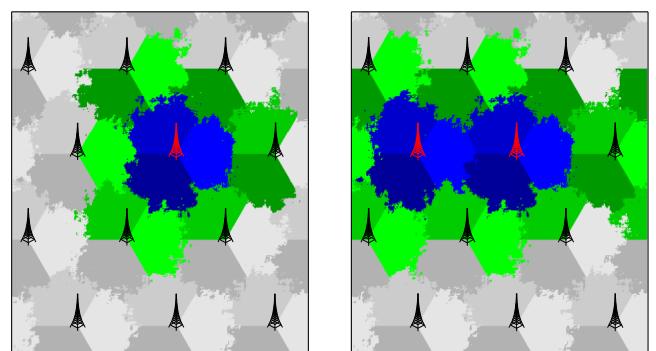
(a) One failing site.　　　　　(b) Two failing sites.

Figure 1: Evaluation areas (blue and green shaded cells) for one and two failing sites.

IV. ALGORITHMS

In this section we elaborate on the algorithms used throughout this paper. More specifically, we describe in Section IV-A

the DBS positioning algorithm proposed in [19], [20], and present in Section IV-B a COC algorithm inspired by [3] for dynamically adjusting the antenna tilts of the cells surrounding the failing sites.

A. DBS positioning algorithm

Suppose that we can deploy N DBSs. We propose a data-driven algorithm that adjusts the (x,y)-coordinates of the N DBSs based on real-time information. For running this algorithm, we use starting positions determined by the method proposed in [29]. From these starting positions, the DBSs try to iteratively improve a so-called control metric (CM), with the assumption that optimizing these CM values also optimizes the overall CSR. For this optimization, we will use a similar approach as in [19], [20]. Specifically, we use the sum of the average load of the N most highly loaded active regular cells of the evaluation area and the load of the DBS cell itself as the CMs. Furthermore, we let the DBSs start at the pre-determined starting positions. At these positions, we measure the CMs, and then iteratively search for a better position with respect to the CM.

For this iterative search, we decide for each DBS whether it moves one meter in the x or y-direction. After this movement, we wait 200 ms to allow for possible handovers, and then start a measurement period of 200 ms to determine the new CMs. Then for each DBS we check whether or not the CM improved. If this is the case, then the DBS continues its movement in that direction until the CM degrades. Otherwise, when the CM already degraded after one step, the DBS starts moving in the opposite direction (so changing its direction by 180 degrees) until the CM degrades again. At that point the DBS starts moving in the other direction (x or y), and repeats the previous steps. A flowchart of this procedure is given in Figure 2.

B. COC algorithm

For the COC algorithm we only consider adjustments of the antenna tilts of cells directly surrounding the failing sites. The focus on antenna tilt adjustments rather than considering (also) adjustments in e.g. reference signal powers is in line with the common radio network planning approach to tailor tilt settings to the inter-site distances, while generally applying uniform reference power settings, and noting that the addressed site failures indeed locally affect the inter-site distances. When adjusting the antenna tilt, the cell should not attract too many additional UEs, as it may then no longer be able to provide adequate service to all its UEs. Moreover, as the UEs that were previously served by the failing sites are further away, they in general have a worse SINR and thus require a larger fraction of the resources. This means that COC aims at serving as many of these UEs as possible while maintaining an acceptable quality of service level for all admitted UEs.

To achieve this, we use a threshold-based COC algorithm inspired by [3] for adjusting the tilts of cells immediately adjacent to the failing sites. For these adjustments, we consider the load of a cell, i.e. the fraction of available cell resources
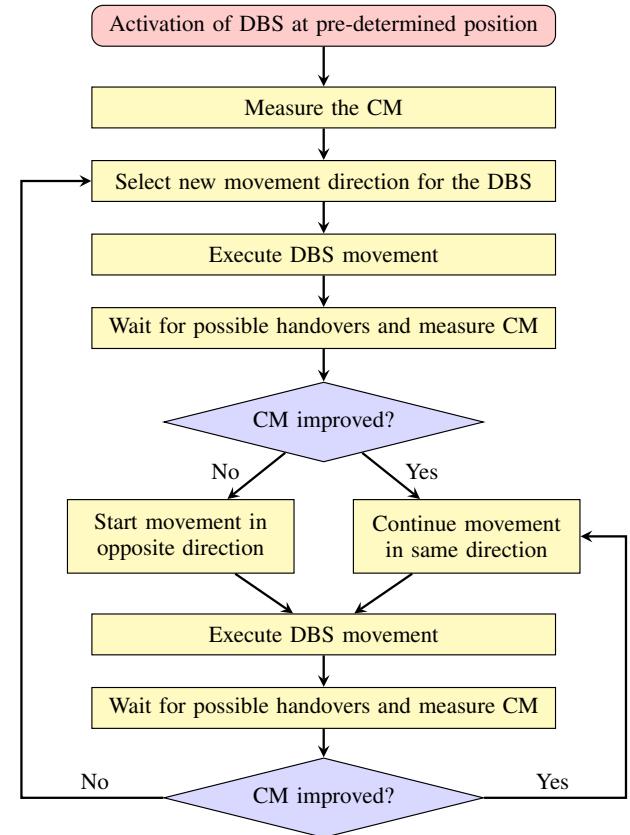

Figure 2: Flowchart of the DBS positioning algorithm, where each DBS follows this procedure.
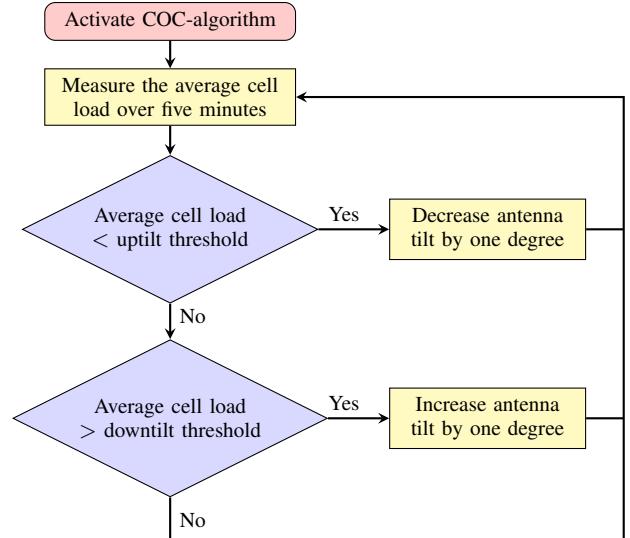

Figure 3: Flowchart of the COC algorithm.

that the served UEs require for satisfactory service. Specifically, we measure the average cell load over a five-minute time interval. If at the end of this time interval the average cell load is below the so-called uptilt threshold, we decrease the tilt of the antenna (uptilt the antenna) of the cell by one

degree. If the average load is above the downtilt threshold, we increase the tilt of the antenna (downtilt the antenna) of the cell by one degree. Finally, if the average cell load falls in between the two thresholds, then the tilt remains the same. In the implementation, we have set a minimum and maximum tilt of 1 and 10 degrees, respectively, to prevent excessive tilt values. A flowchart of the algorithm is presented in Figure 3.

The reasoning behind this algorithm is as follows: we measure the cell load over a five-minute time window and then update the tilt at the end of this time window to respond to persistent changes in the environment, while avoiding over-reaction to small fluctuations such as when a UE is admitted or leaves. The rationale behind uptilting the antenna under low traffic loads is that under low loads, the cell can indeed expand its coverage and handle the additionally attracted load. The reasoning to downtilt an antenna is that a heavily loaded cell aims to reduce its load by decreasing its coverage area and therefore steers traffic towards other cells.

V. PERFORMANCE EVALUATION

In this section we evaluate the performance of the proposed algorithms. To do this we first tune the proposed COC algorithm by selecting suitable threshold values for it in Section V-A and then evaluate the performance of the deployment of DBSs in the presence of COC in Section V-B.

A. Determining suitable COC threshold values

To determine suitable threshold values for the COC algorithm, we consider downtilt threshold values in $\{0.7, 0.75, \ldots, 1\}$ and uptilt threshold values in $\{0, 0.05, \ldots, 0.5\}$, for eighteen scenarios with up to four deployed DBSs. To examine the impact of these threshold values, we conduct various simulation experiments where we consider all combinations of the aforementioned thresholds. In these simulations, besides the tilt adjustments, the deployed DBSs move around according to the algorithm proposed in [20]. To calculate the CSR, we take the average CSR over 25 independent simulation runs where the CSR of each run considers a time period representing four hours starting from an equilibrium state. In Figure 4 we plot the resulting CSR for the deployment of zero and three DBSs for both the DU-1-60-150-8 and RU-60-1000-40 scenarios, respectively.

In this figure, we see that the optimal combination of threshold values depends on both the scenario and the number of deployed DBSs. For example, in the DU-60-150-8 scenario without DBSs the optimal down- and uptilt thresholds are 1 and 0, respectively, which means that the tilts are not adjusted and therefore kept at the default values. For the same scenario with three DBSs the optimal thresholds are 0.8 and 0.15, respectively, which implies that the antenna should be uptilted when the load drops below 0.15 and downtilted when the load exceeds 0.8. In order to show the optimal configuration of the threshold values for all considered scenarios we plot in Figure 5 the optimal uptilt and downtilt thresholds for each scenario with zero up to four deployed DBSs, depicted consecutively with distinct markers from left to right for each scenario.

In this figure we see that there is quite some variation in the optimal threshold values for the different scenarios and deployed number of DBSs. However, in general it is not likely that operators will tune the threshold values for all possible scenarios and number of deployed DBSs. Assuming that an operator prefers a limited number of configurations for the COC algorithm, based on the considered scenarios in Figure 5, we propose two sets of down- and uptilt threshold values: (0.9, 0.2) for dense urban scenarios and (0.9, 0.3) for rural scenarios, respectively.

B. Performance evaluation

To evaluate the performance of the combination of dynamic DBS deployment and COC algorithm, we compare the CSR performance for the dynamic deployment of up to four DBSs in combination with: i) No COC, where the tilts are fixed at default values. ii) The considered COC algorithm configured with the environment-specific thresholds proposed at the end of Section V-A. iii) The considered COC algorithm configured with the optimal threshold values shown in Figure 5. Let us now compare the performance of the three approaches in Figure 6. In this figure we consider various scenarios, where for each scenario we evaluate the call failure rate (CFR $= 1 - $ CSR) performance with zero up to four deployed DBSs, depicted consecutively with distinct markers from left to right for each scenario.

We see that in most scenarios the case with the COC algorithm configured with the proposed thresholds outperforms the setting without COC, especially in the rural scenarios. However, we note that in the dense urban scenarios, when no DBSs are deployed, the approach without COC often performs better than the approach with COC based on the proposed thresholds for dense urban environments. A possible explanation for this is that the degree of antenna downtilting induced at the surrounding cells under the proposed thresholds is typically undesirably large in these scenarios. In the former case without any deployed DBSs, the downtilting yields a coverage degradation with no DBS to compensate for that. In the latter case with a relatively high number of failing sites the coverage-affected area is likely too large for the deployed DBSs to handle, particularly when the surrounding cells reduce their coverage by further downtilting their antennas. Hence for these and similar scenarios, i.e. where the effective area of coverage loss is expected to be too large for the set of deployed DBSs to handle, it may be good to apply different COC thresholds.

We further observe that for the given scenarios the most effective means to alleviate the performance challenges caused by site failures is the deployment of a sufficient number of DBSs, and to a lesser degree the use of a COC mechanism. This can for example be seen by considering that in most cases the addition of a DBS yields a bigger reduction in CFR than the addition of the COC algorithm configured with the optimal thresholds. Nevertheless, COC can play a significant role, in particular during the time between a base station failure and the arrival of DBSs.

(a) DU-1-60-150-8 without DBSs.

(b) DU-1-60-150-8 with three DBSs.

(c) RU-1-60-1000-40 without DBSs.

(d) RU-1-60-1000-40 with three DBSs.
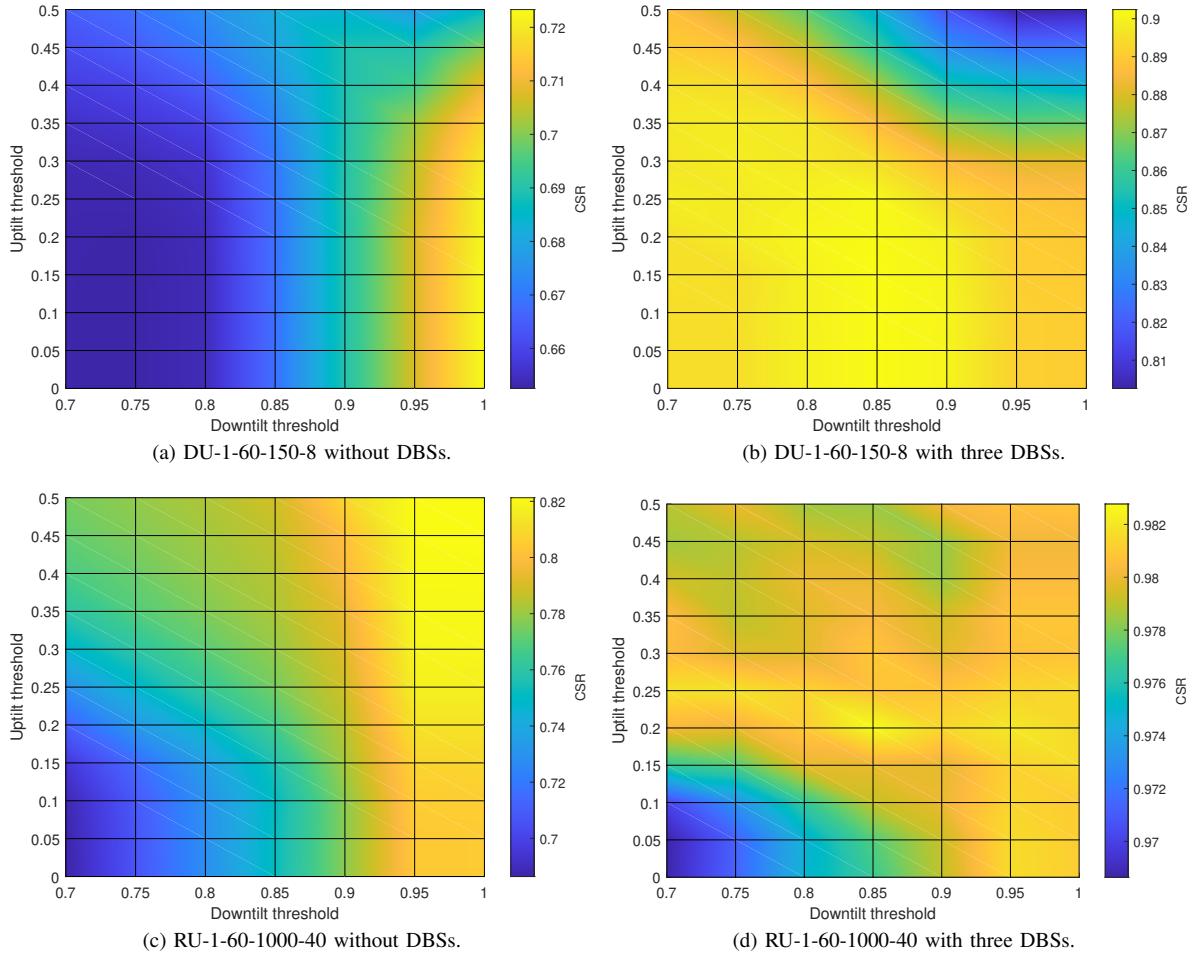
Figure 4: CSR for different combinations of the threshold values for the DU-1-60-150-8 and RU-1-60-1000-40 scenarios without and with three DBSs.

From these results, it seems that the two control loops for the DBS positioning and COC adjustments do not affect each other too much. A possible explanation for this is that the two control loops work on different time scales, i.e. seconds for the position adjustments, while the tilt adjustments occur at most once every five minutes.

VI. CONCLUSION

In this paper we have investigated the joint use of COC and dynamically deployed DBSs to restore network performance in case of site failures. An extensive simulation study showed that with proper parameter settings the algorithms for COC and DBS deployment can work well together. In particular, while COC on its own is mostly not able to bring the call success rate back to its original level after failure of one or more sites, it can help to significantly reduce the number of DBSs that need to be deployed to achieve this.

The COC and DBS positioning algorithms used in this paper involve two separate control loops without any explicit coordination between them. Even though they seem to work well together as mentioned above, we still expect that their joint performance can be improved by developing more tightly integrated solutions. Possible development directions include developing: i) a COC algorithm that does not rely on pre-determined up- and downtilt threshold values, but instead determines these in a dynamic/data-driven way, effectively responding to the (im)balance between the size of the affected area and the (known) number of deployed DBSs; or ii) a COC algorithm that takes the positions of the DBSs and the azimuths of the still operational cells with respect to the disaster-struck area explicitly into account.

REFERENCES

[1] M. Amirijoo, L. Jorguseski, R. Litjens and R. Nascimento, "Effective-ness of Cell Outage Compensation in LTE Networks", in *2011 IEEE Consumer Communications and Networking Conference (CCNC)*, 2011.

[2] M. Mozaffari, W. Saad, M. Bennis, Y.-H. Nam and M. Debbah, "A tutorial on UAVs for wireless networks: applications, challenges, and open problems", in *IEEE Communications Surveys & Tutorials*, vol. 21, no. 3, 2019.

[3] M. Amirijoo, L. Jorguseski, R. Litjens and L.C. Schmelz, "Cell Outage Compensation in LTE Networks: Algorithms and Performance Assessment", *2011 IEEE 73rd Vehicular Technology Conference (VTC Spring)*, 2011.

[4] G. Micallef, P. Mogensen and H. Scheck, "Cell Size Breathing and Possibilities to Introduce Cell Sleep Mode", *2010 European Wireless Conference (EW)*, 2010.
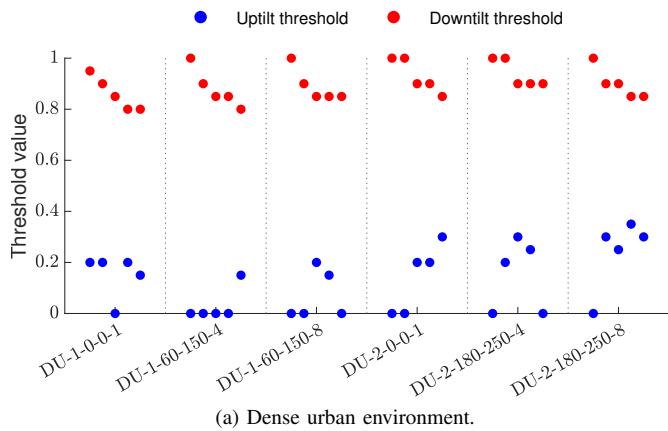
(a) Dense urban environment.
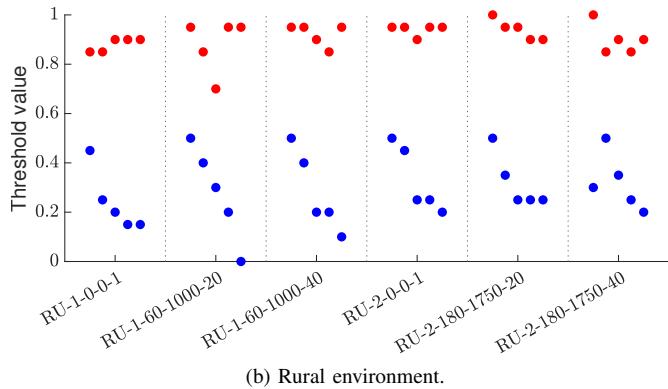
(b) Rural environment.

Figure 5: Optimal combinations of threshold values for different scenarios with zero (left) up to four (right) deployed DBSs.


(a) Dense urban environment.

(b) Rural environment.

Figure 6: CFR for different scenarios with zero (left) up to four (right) deployed DBSs.

[5] I. de la Bandera, P. Muñoz, I. Serrano and R. Barco, "Adaptive Cell Outage Compensation in Self-Organizing Networks", *IEEE Transactions on Vehicular Technology*, vol. 67, no. 6, 2018.

[6] S. Adel, K. Muhammed, A. Abdallah, M. Rida, A. Morsy, G. Nasser, A. Khattab, A. Taha and H. El-Akel, "Cell Outage Compensation Using Q-learning for Self-Organizing Networks", *2021 International Conference on Microelectronics (ICM)*, 2021.

[7] L. Kayili and E. Sousa, "Cell Outage Compensation for Irregular Cellular Networks", *2014 IEEE Wireless Communications and Networking Conference (WCNC)*, 2014.

[8] W. Li, P. Yu, M. Yin and L. Meng, "A Distributed Cell Outage Compensation Mechanism Based on RS Power Adjustment in LTE Networks", *China Communications*, vol. 11, no. 13, 2014.

[9] X. Yang, P. Yu, L. Feng, F. Zhou, W. Li, and X. Qiu, "A Deep Reinforcement Learning based Mechanism for Cell Outage Compensation in 5G UDN", *2019 IFIP/IEEE Symposium on Integrated Network and Service Management (IM)*, 2019.

[10] P.V. Klaine, J.P.B. Nadas, R.D. Souza and M.A. Imran "Distributed drone base station positioning for emergency cellular networks using reinforcement learning", *Cognitive Computing* vol. 10, 2018.

[11] R. de Paula Parisotto, P.V. Klaine, J.P.B. Nadas, R.D. Souza, G. Brante and M.A. Imran, "Drone base station positioning and power allocation using reinforcement learning", *2019 ISWCS*, Oulu, Finland, 2019.

[12] E. Kalantari, H. Yanikomeroglu and A. Yongacoglu, "On the number and 3D placement of drone base stations in wireless cellular networks", *2016 IEEE VTC-Fall*, Montreal, Canada, 2016.

[13] W. Shi, J. Li, W. Xu, H. Zhou, N. Zhang, S. Zhang and X. Shen, "Multiple drone-cell deployment analyses and optimization in drone assisted radio access networks", in *IEEE Access*, vol. 6, 2018

[14] T. Akram, M. Awais, R. Naqvi, A. Ahmed and M. Naeem, "Multicriteria UAV base stations placement for disaster management", in *IEEE Systems Journal*, vol. 14, no. 3, 2020.
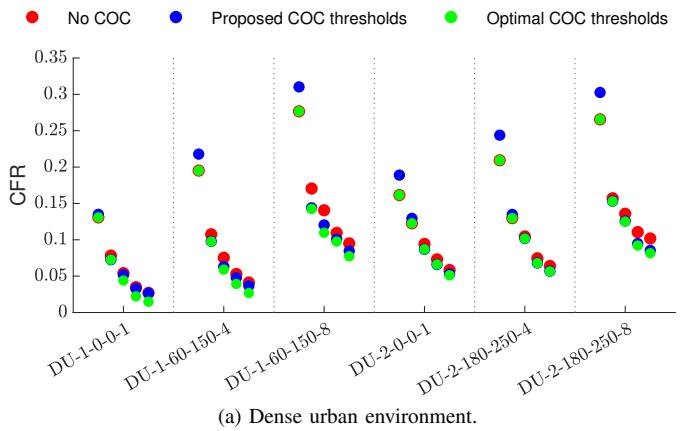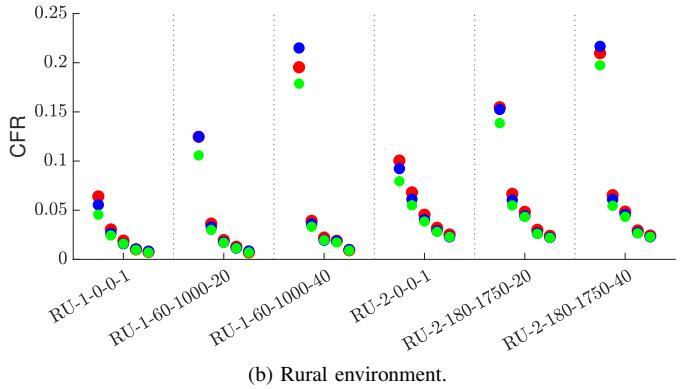
[15] F. Al-Turjman, J.P. Lemayian, S. Alturjman and L. Mostarda, "Enhanced deployment strategy for the 5G drone-BS using artificial intelligence", in *IEEE Access*, vol. 7, 2019.

[16] X. Li, "Deployment of drone base stations for cellular communication without apriori user distribution information", *2018 37th Chinese Control Conference (CCC)*, 2018.

[17] H. Ahmadi, K. Katzis and M. Z. Shakir, "A novel airborne self-organising architecture for 5G+ networks", *2017 IEEE VTC-Fall*, 2017.

[18] D. Prado, S. Inca, D. Martín-Sacristán and J.F. Monserrat, "Comparison of optimization methods for aerial base station placement with users mobility", *2019 EuCNC*, Valencia, Spain, 2019.

[19] T.R. Pijnappel, J.L. van den Berg, S.C. Borst and R. Litjens, "Online Positioning of a Drone-Mounted Base Station in Emergency Scenarios", *IEEE Transactions on Vehicular Technology*, 2023.

[20] T.R. Pijnappel, J.L. van den Berg, S.C. Borst and R. Litjens, "Data-Driven Positioning of Drone Base Stations in Emergency Scenarios", *2024 IEEE VTC-Fall* (to appear), Washington DC, USA, 2024.

[21] 3GPP TR38.901: "Study on channel model for frequencies from 0.5 to 100 GHz", *3GPP Technical Report*, v16.1.0, 2019.

[22] F. Gunnarsson, M.N. Johansson, A. Furuskär, M. Lundevall, A. Simonsson, C. Tidestav and M. Blomgren, "Downtilted base station antennas - a simulation model proposal and impact on HSPA and LTE performance", *2008 IEEE VTC-Fall*, Calgary, Canada, 2008.

[23] Ericsson. "Ericsson Antenna System Catalog 2021", 2021, pp 487-494.

[24] ITU-R, Rec. P1410-2 "Propagation data and prediction methods for the design of terrestrial broadband millimetric radio access systems", P Series, *Radiowave Propagation*, 2003.

[25] A. Al-Hourani, S. Kandeepan and S. Lardner, "Optimal LAP altitude for maximum coverage", in *IEEE Wireless Communications Letters*, vol. 3, no. 6, 2014.

[26] R. Fraile, J. F. Monserrat, J. Gozálvez and N. Cardona, "Mobile radio bi-dimensional large-scale fading modelling with site-to-site cross-

correlation", in *European Transactions on Telecommunications*, vol. 19, 2008.

[27] 3GPP TR36.942: "Evolved universal terrestrial radio access (E-UTRA); radio frequency (RF) system scenarios", *3GPP Technical Report*, v16.0.0, 2020.

[28] A. Al-Hourani, S. Kandeepan and A. Jamalipour, "Modeling air-to-ground path loss for low altitude platforms in urban environments", *2014 IEEE GLOBECOM*, Austin, USA, 2014.

[29] T.R. Pijnappel, J.L. van den Berg, S.C. Borst and R. Litjens, "Analytical Approach for Optimal Deployment of Drone Base Stations in Cellular Networks", *ICC 2023 - IEEE International Conference on Communications*, 2023.